Azimuthal instabilities in annular combustion chambers

By P. Wolf*†, G. Staffelbach†, R. Balakrishnan‡, A. Roux¶ AND T. Poinsot‖

Large Eddy Simulations (LES) of a full annular helicopter gas turbine combustor have been performed. Emphasis is placed on the azimuthal mode that often appears in real configurations. The current LES are shown to capture these self-excited modes, with limited impact of the grid resolution. The structure of the azimuthal mode is discussed and shown to be described by a simple analytical model. The acoustic field corresponds to a standing mode pattern along with a slowly turning behavior that is due to a convective overall swirling motion in the chamber. The Flame Transfer Function (FTF) is then extracted from the full multi-burner LES results and compared to both Proper Orthogonal Decomposition (POD) analysis and a pulsated single sector LES. Good agreement is found regarding the delay between velocity and heat release perturbations.

1. Introduction

Azimuthal modes are instabilities appearing in annular combustion chambers of many gas turbines: they can lead to vibrations and structural damage (Lieuwen & Yang 2005) and should be eliminated at the design stage, something which is impossible today because fundamental issues in terms of mechanisms and modeling are still open:

- Why do these modes appear?

The models used to predict stability in annular chambers are usually based on a one-dimensional network view of the chamber (Dowling 1995; Lohrmann *et al.* 2003; Schuermans *et al.* 2003) in which each burner is only influenced by the flow rate fluctuation it is submitted to by the azimuthal acoustic mode. All burners are supposed to have the same transfer function (i.e. the same relation between inlet burner velocity u' and total heat release rate fluctuations q'). This may not be the case in practice: in liquid-fueled rocket engines or more generally in burners containing multiple jets (Poinsot *et al.* 1987), the interaction between neighboring flames can lead to instability. This may happen in gas turbines too and require other modeling approaches than the existing ones.

- What is the structure of these modes?

In annular combustion chambers, the first (and sometimes second) azimuthal acoustic mode is often the strongest mode (Stow & Dowling 2001; Krebs *et al.* 2002; Schuermans *et al.* 2006). Azimuthal modes can appear as standing modes or rotating modes and both are observed in gas turbines. Schuermans *et al.* (2003, 2006) propose a non-linear theoretical approach showing that standing modes can be found at low oscillation amplitudes but that only one rotating mode is found for large amplitude limit cycles. Other

† CERFACS, CFD team, 42 Av Coriolis, 31057 Toulouse, France
‡ ALCF, Argonne National Laboratory
¶ CTR, Stanford University
‖ IMF Toulouse, INP de Toulouse and CNRS, 31400 Toulouse, France

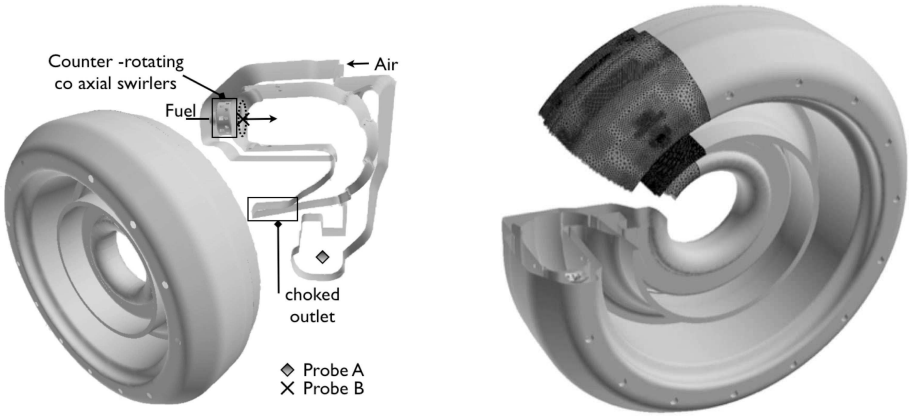

FIGURE 1. Gas turbine geometry and mesh.

explanations can be found in linear approaches: standing modes would appear only in perfectly axisymmetric configurations while any symmetry modification would lead to rotating modes (Sensiau *et al.* 2009). Opposite theories are found in Noiray *et al.* (2010) showing that the question remains controversial.

Using experiments to study these issues is difficult because multi burner combustion chamber rigs are expensive and rare. A new approach is now possible using massively parallel computations and Large Eddy Simulation (LES). Multiple studies have demonstrated the power of LES in configurations which are very close to single sector domains of real gas turbine chambers (Moin & Apte 2006; Mahesh *et al.* 2006; Schmitt *et al.* 2007). Such LES solvers can predict instabilities in reacting flow configurations (Poinsot & Veynante 2005; Selle *et al.* 2004). By running them on a massively parallel machine (typically 16,000 processors), it is now possible to compute a full combustion chamber with 15 to 24 sectors (and not a single sector only) and investigate the mechanisms leading to the growth of azimuthal instabilities. In the present study, LES is used to compute the reacting unstable flow within a full combustion chamber of an helicopter turbine (Staffelbach *et al.* 2009; Wolf *et al.* 2009) equipped with fifteen burners (Fig. 1).

2. Configuration and numerical set up

The combustion chamber is composed of fifteen burners. Each burner contains two co-annular swirlers. The fuel injectors are placed in the axis of the swirlers. To avoid uncertainties associated with the boundary conditions (especially on inlet and outlet impedances) the chamber casing is also computed. The computational domain starts after the inlet diffuser and ends at the throat of the high pressure stator where the choked flow is explicitly computed by the solver, avoiding uncertainties on acoustic impedances. The air and fuel inlets use non-reflective boundary conditions (Poinsot & Lele 1992). The air flowing at 578 K in the casing feeds the combustion chamber through the swirlers, films and dilution holes.

The reacting flow in the combustor of Fig. 1 is investigated using a compressible LES solver (Gourdain *et al.* 2009): simulations are performed by first computing a single sector, duplicating the result 14 times around the turbine axis, and then letting the computation evolve to the most amplified oscillation mode. No forcing is added: the LES

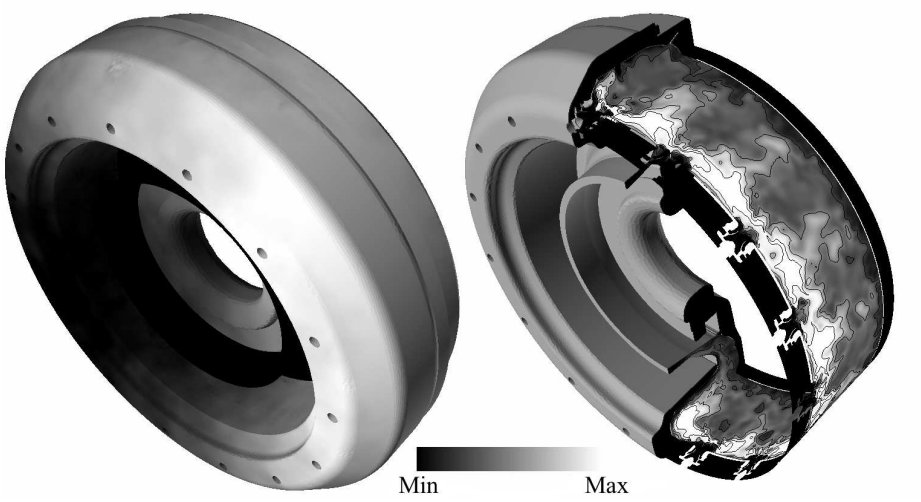

FIGURE 2. Flow visualization. Left: pressure field on the combustor skin. Right: temperature field with temperature isocontours on a cylindrical plane passing through the B_i probes.

captures (or not) the oscillation modes of the combustor without any external excitation (Staffelbach *et al.* 2009). In most cases, a transient period of growth is followed by the formation of azimuthal modes in the combustion chamber. These modes cause the flames to oscillate both azimuthally and longitudinally, causing periodic flashbacks inside the injectors, as illustrated by Fig. 2.

3. Mean swirl, turning and standing modes

Even though the configuration of the swirlers is axi-symmetric, the swirl imposed in each burner makes one rotation direction preferential, leading to the existence of a mean swirling velocity in the combustor. The azimuthal mode that form in the chamber is primarily composed of two waves traveling in different directions. These two components induce an important difference between the co-rotating wave (turning in the direction of the swirl induced by the injectors) called here the "+" wave and the counter-rotating one, called the "-" wave. To first order, the + wave turns at a velocity $c + V_\theta$ where V_θ is the mean swirl velocity and c the mean sound speed in the chamber while the $-$ wave turns at $c - V_\theta$. The mean swirling velocity V_θ is small compared to the sound speed c: average typical swirl velocities of 10 m/s are observed in the LES. This allows the effect of the sound speed to be separated from the effect of the swirl velocity. The main azimuthal mode is observed at a carrier frequency of the order of $c/2\pi R$ and it is modulated by a lower frequency (of the order of $V_\theta/2\pi R$).

To illustrate this point and ease the interpretation of LES results in the following, a simple model is described here to express the pressure oscillations p' resulting from the combination of the + and $-$ waves in an annulus of radius R where the period and the angular frequency of the azimuthal mode without swirling flow are $T_{azi} = 2\pi R/c = 2\pi/\omega$ and $\omega = c/R$ respectively. The pressure signal may then be written as:

$$p' = \hat{p}e^{(-i\omega t)} = \left[A_+ e^{i(\theta - V_\theta t/R)} + A_- e^{i(-\theta + V_\theta t/R)}\right] e^{-i\omega t} \tag{3.1}$$

where θ is the angle measuring a point position along the azimuthal direction. The $V_\theta t/R$

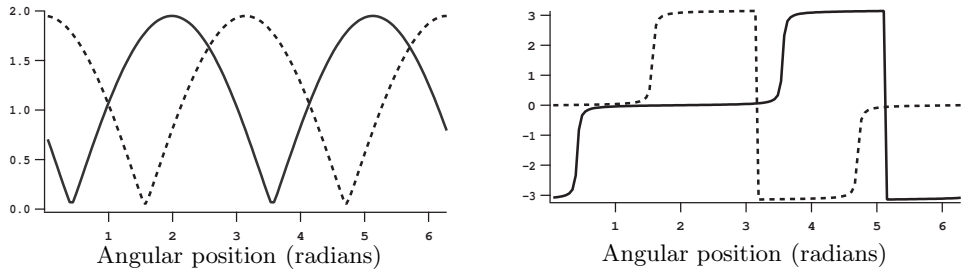

FIGURE 3. Pressure perturbations modulus (left) and phase (right) versus angle at two times separated by a time equal to 25 periods of the azimuthal mode in an ideal annular chamber with $R = 0.176$ m (radius), $c = 790$ m/s (sound speed) and $V_\theta = 10$ m/s (average swirl velocity) (Eq. 3.1).

terms are induced by the mean swirl convection at speed V_θ. They change very slowly compared to the ωt term so that a structure can be defined for p' by observing it over a few periods of the short (acoustic) time: this structure then changes over long (convective) times. Typically, gas turbine experts observe standing azimuthal modes (oscillating at hundreds of Hertz) where the pressure nodes are turning very slowly (depending on the configuration, one full rotation could take as long as a few seconds to a few hours). The period required for a complete rotation of the structure is simply $2\pi R/V_\theta$ or T_{azi}/M_a where $M_a = V_\theta/c$ is the Mach number of the swirling flow component.

This observation makes the analysis of azimuthal modes more complicated: a standing mode (observed over a few periods) can exhibit a structure which rotates slowly (with the swirl velocity). Such a mode is not a 'turning' mode where the pressure field rotates with the sound speed. When using LES, sampling over very long times is difficult so that observing a full rotation of such a structure is costly. In the present LES, the oscillations were computed for 130 ms corresponding to 100 cycles of the azimuthal mode but only slightly more than one rotation of the rotating structure. However, as soon as the rotation effect due to the mean swirl component has been identified, the structure can be studied over a few periods of the azimuthal mode, knowing that it will rotate with the mean swirl velocity V_θ if one observes it for a long time. This rotation will not change the fundamental mode structure observed at shorter times.

As an example, Fig. 3 shows the mode structure (modulus and phase of $\hat{p}_i$†) computed at short times using Eq. 3.1 at two instants t_i $(i = 1, 2)$ separated by 25 periods of the azimuthal mode T_{azi} in a case where $A_+ = 1$, $A_- = 0.95$ and $V_\theta = 10$ m/s:

$$\hat{p}_i = A_+ e^{i(\theta - V_\theta t_i/R)} + A_- e^{i(-\theta + V_\theta t_i/R)} \tag{3.2}$$

where $t_2 = t_1 + 25T_{azi}$. As expected, the mode keeps the same structure, very similar to a standing mode, but it has turned slowly between the two instants, shifting the pressure nodes and antinodes by approximately $\pi/2$.

4. Effects of mesh resolution

Table 1 presents the three meshes used to verify grid refinement effects. The objective of this test was to compare the mean flow obtained on the three grids but also the self-

† The exact expression for the phase ϕ_1 plotted in Fig. 3 is the difference between the argument of p' (which depends on t in Eq. 3.1) and its value at a fixed θ_0 which is fixed here to $\theta_0 = 0$. The plotted phase is $\phi_1 = arg(p') - arg(p'(\theta = 0) = arg(p') + \omega t = arg(\hat{p})$.

Grid	Number of points	Number of cells	Time step (s)	Elapsed time for one azimuthal cycle (hours)
Coarse	6 916 125	37 696 365	$6\ 10^{-8}$	2h 10min
Medium	16 466 145	93 147 720	$3\ 10^{-8}$	11h 15min
Fine	54 954 975	336 078 255	$3\ 10^{-8}$	33h 30min

TABLE 1. Characteristics of unstructured meshes used for LES and corresponding CPU time on a BlueGene machine using 16384 processors.

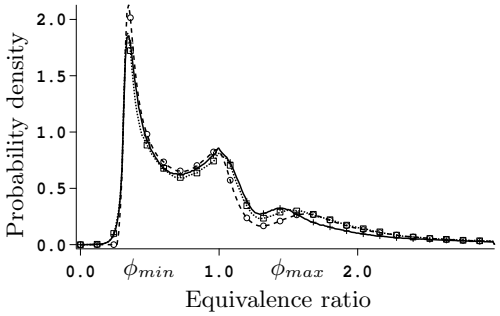

FIGURE 4. Mesh independency tests: probability density function of equivalence ratio for the three considered meshes: coarse (solid lines with crosses), medium (dotted lines with squares) and fine (dashed lines with circles).

amplified modes. Note that CPU time depends not only on the number of grid points but also on the time step, as the LES code used throughout this study is explicit.

Runs are first started on the coarse mesh, the simulation is then continued using the medium and fine grids. The mean flow shows very limited changes. In particular, combustion behaves similarly on the three grids. Figure 4 presents the probability density function (PDF) of the resolved equivalence ratio in reacting zones obtained on all three meshes. Most of the combustion takes place in lean premixed zones, with a strong peak at an equivalence ratio of ϕ_{min}. Another peak is located at $\phi = 1$ and stems from the presence of diffusion flamelets. A weaker peak appears around ϕ_{max} and corresponds to rich premixed flames created close to the fuel injection. All peaks are unaffected by grid refinements. More interestingly for our study, the unsteady activity remained the same on the refined grid (Fig. 5 shows the transition from the coarse to the fine grid): the instability cycle continued at the same frequency and with the same amplitude showing that the results depend only weakly on the mesh.

5. Mode structure obtained by LES

The LES results on the coarse grid are analyzed here over a large number of cycles (50) to investigate the mode structure. First, Fig. 6 displays the mode structures obtained

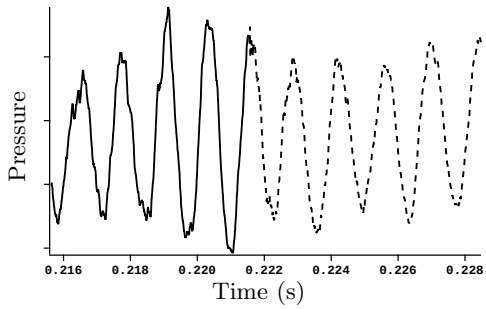

FIGURE 5. Mesh independency tests: pressure perturbations at probe B_1. The simulation is run on the coarse mesh (solid line) until $t = 0.2215$ ms. It is then continued on the fine grid (dashed line).

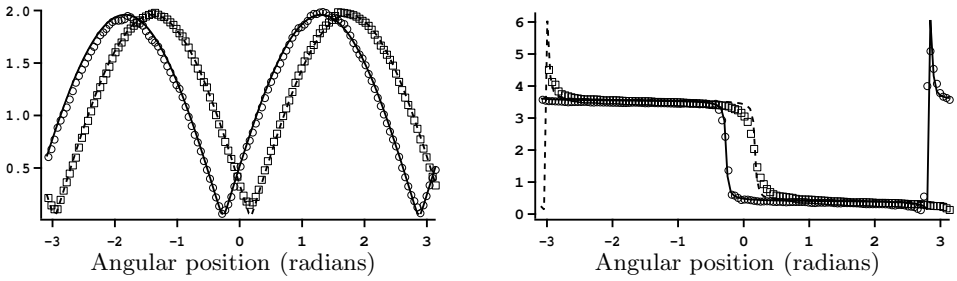

FIGURE 6. LES results: pressure perturbations modulus (left) and phase (right) at two times $t_1 = 0.143$ s (circles) and $t_2 = 0.153$ s (squares). A fit using Eq. 3.1 is also added with $A_-/A_+ = 0.96$ (solid and dashed lines).

at two instants of the simulation $t_1 = 0.143$ s and $t_2 = 0.153$ s. To construct these structures, seven cycles at 750 Hz are sufficient. Figure 6 demonstrates that a standing mode is observed and that this standing mode is rotating slowly. The rotation velocity is 44 rad/s corresponding to a mean swirl velocity $V_\theta \approx 7.8$ m/s in the combustion chamber. This value matches the levels measured in the LES.

Figure 6 can be used to deduce A_+ and A_- (as defined in Eq. 3.1). In the present case, the best fit of Eq. 3.1 to the LES results corresponds to $A_-/A_+ = 0.96$. This mode is slowly turning because of the mean swirl produced in the chamber. No purely turning mode (for which either A_+ or A_- must be zero) is observed. Schuermans *et al.* (2006) suggest that these standing (or convectively turning) modes are less likely to be found when the limit cycle is reached than rotating modes (in the sense of acoustically rotating). The outcome of the present study is not consistent with recent developments by Noiray *et al.* (2010) who predicts standing modes in asymmetrical configurations but purely rotating modes in symmetrical ones. Further studies will require LES of non axisymmetric cases to see whether the standing mode is replaced by a purely turning mode or not.

6. POD analysis of self-excited azimuthal modes

The previous section addressed the structure of the mode (standing or turning). In the present section, the LES results are decomposed using Proper Orthogonal Decomposition (POD). POD is aimed at obtaining low-dimensional approximate descriptions of high-

dimensional phenomena, such as turbulent flows (Lumley 1967; Berkooz *et al.* 1993). The main interest of POD is to isolate the most energetic mode and analyze it without having to take the rest of the unsteady activity into account (Roux *et al.* 2007). For example, computing Flame Transfer Function should be simpler using POD.

In our study, snapshot POD is considered: a collection of observations (or snapshots) $q(x, t_n)$ evenly spaced in time is considered over a spatial domain Ω. The considered flow quantity is then rewritten as:

$$\hat{q}(x,t) = \sum_{n=1}^{N} a_n(t)\Psi_n(x) \tag{6.1}$$

where $a_n(t)$ is the temporal expansion coefficient and $\Psi_n(x)$ is the spatial eigenvector corresponding to the nth POD mode. To determine the POD mode, the following integral eigenvalue equation is considered:

$$\int_{T_{sim}} C(t,t')a_n(t')dt' = \lambda_n a_n(t) \tag{6.2}$$

where T_{sim} is the duration of the simulation, $C(t, t')$ is the autocorrelation function for q and λ_n is the nth eigenvalue.

POD analysis has been applied to extract the most energetic modes from velocity, pressure and heat release fluctuations from 150 snapshots discretizing 7 cycles of the carrier mode. It provides an energetic classification of the different modes within the simulation. When applied to the acoustic energy, POD yields first a pair of eigen-functions at the same frequency as the azimuthal mode. Assuming that the mean swirl has a constant effect on the evolution of the azimuthal mode†, Eq. 3.2 can be used to extract the spatial and temporal structure of the first two POD pressure modes. It reads:

$$p' = \underbrace{\left(A^+ + A^-\right)\cos\left(\theta - V_\theta t/R\right)}_{\Psi 1(x)} \times \underbrace{\cos\left(\omega t\right)}_{a_1(t)} + \underbrace{\left(A^+ - A^-\right)\sin\left(\theta - V_\theta t/R\right)}_{\Psi 2(x)} \times \underbrace{\sin\left(\omega t\right)}_{a_2(t)} \tag{6.3}$$

Thus, POD recovers the propagating nature of the azimuthal self-excited standing mode which is composed of two traveling waves. As described in Sec. 3, the current simulation exhibits waves such as $A^+ - A^- \approx 0.05 \times A^+$: the second wave is damped compared to the first one. In the following, the study focuses on the latter.

The structure of the most energetic modes of pressure, velocity and heat release fluctuations is displayed in Fig. 7. The diagnostic confirms the importance of the self-excited azimuthal mode on the behaviour of the flame: the presence of nodes and anti-nodes of pressure induces fluctuations of mass flow rate within the swirler which are then responsible for the oscillation of heat release downstream. These events occur shifted in time and can be described using the temporal expansion coefficients $a_n(t)$, as shown by Fig. 8. The delay between velocity and heat release can then be extracted so as to assess the response of the burner to a velocity fluctuation.

7. Evaluation of FTFs (Flame Transfer Function)

The most important quantity to predict stability of a combustor is its Flame Transfer Function (FTF) which measures the flame response to a fluctuation of the inlet flow rate.

† $V_\theta t/R \approx C^{te}$ if $T_{sim} << R/V_\theta$

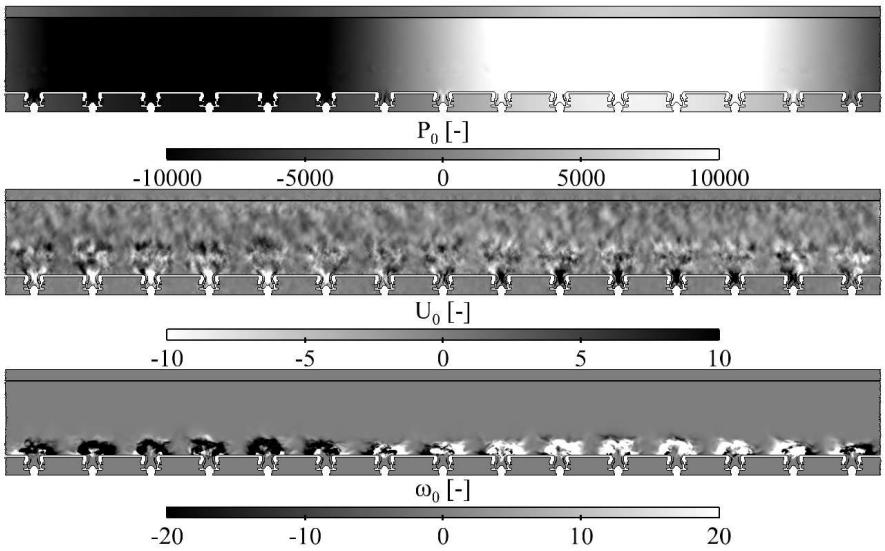

FIGURE 7. Amplitude fields as obtained from POD. Most energetic mode. From top to bottom: pressure, axial velocity and heat release fluctuations.

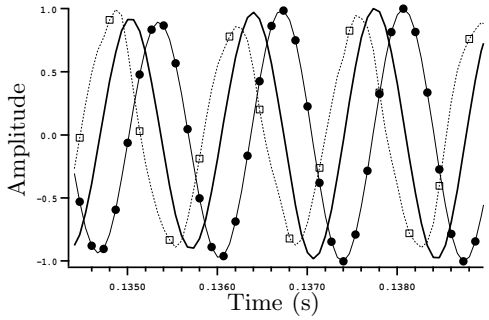

FIGURE 8. Temporal evolution of the first temporal expansion coefficient of pressure (solid), axial velocity (square) and heat release (circle) fields as obtained from POD.

The FTF is obtained by measuring the transfer function between the variation of total heat release q' versus inlet velocity u'. This leads to the definition of a gain n and a delay τ defined by:

$$F(\omega) = \frac{(q'/\bar{q})}{(u'/\bar{u})} = ne^{|i\omega\tau|} \tag{7.1}$$

where $\bar{f}$ denotes time averaging. The delay τ controls the stability of the combustor (Lieuwen *et al.* 2001; Sensiau *et al.* 2009; Morgans & Dowling 2007).

Three separate methods were used here to evaluate the delay of the FTF which is the most important parameter controlling stability.

• The FTF delay τ was first computed using a single-burner computation where the air inlet was forced at the frequency of the azimuthal mode, following the procedure discussed in Kaufmann *et al.* (2002).

• In parallel, the LES signals of the multi-burner self-excited simulations were post processed to obtain the FTF delay between the heat release perturbations (measured in

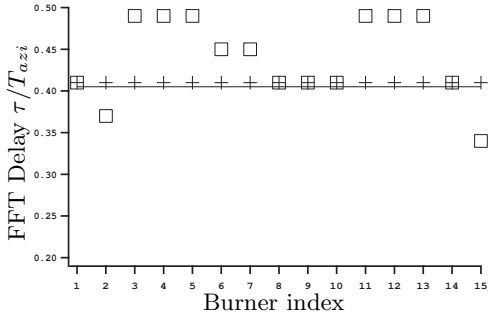

FIGURE 9. Comparison of FTF delays τ/T_{azi} obtained on a single forced sector (solid line) and on the multi-burner LES using the raw LES signals (squares) and the POD analysis using the most energetic mode (crosses).

each individual sector) and the velocity perturbations at the corresponding swirler. In the considered multi burner turbine, the FTF is defined for each of the 15 sectors.

• The POD results of the multi-burner LES were used to obtain the FTF delay by evaluating it for the most energetic mode.

For all cases, the inlet velocity was defined in the same way: it is the average normal velocity on a cylinder surrounding the swirler. The flame is never seen in this position so that it is a flame independent evaluation of the flow rate perturbations passing through the swirler. This procedure allows to address two questions:

• Is the FTF computed using only one forced sector the same as the FTF observed in the full self-excited computation? If it is, this is a useful procedure because the single sector case is much faster to compute.

• Is the POD analysis a proper technique to construct FTF? This would ease FTF analysis in very complex cases.

Fig. 9 displays the results of this analysis as a function of burner position. The average delay obtained by all methods is of the order of $\tau/T_{azi} = 0.4$. In the full multi-burner LES, variations are observed for burners which are close to pressure nodes and for which perturbations are smaller, leading to reduced signal-to-noise ratios. The forced single burner delay is $\tau/T_{azi} = 0.405$ and corresponds very well to the average LES data on the multi-burner self-excited LES. Finally, POD results show that the delay is mainly controlled by the first mode. This mode is the standing mode observed in Fig. 6. When using this mode only, POD gives the same delay for all burners $\tau/T_{azi} = 0.405$ which is very close to the single-burner LES results. These results show that performing a forced single burner simulation is a good method to obtain the FTF delay and that POD is an efficient way to evaluate delays in the multi-burner simulation where it allows to isolate the first most energetic mode and measure its FTF in a reliable and fairly straightforward manner. Using the raw LES data on the other hand leads to some scatter on the results because burners located at pressure nodes exhibit low signal-to-noise ratios.

8. Conclusions

LES of self-excited azimuthal oscillations in a full realistic combustion chamber have been used to verify mesh independency, analyze the mode structure (using LES signals but also POD analysis) and measure flame delays. Results show that the LES is fairly mesh independent and that the unstable mode is a standing mode which can be described by simple acoustic models. This structure is rotating at the mean swirl speed. The flame

delays of all sectors were shown to be the same and equal to the value given by a single sector forced simulation at the azimuthal frequency. POD was used to isolate the azimuthal mode and evaluate its delay with precision.

Acknowledgments

This research used resources of the Argonne Leadership Computing Facility at Argonne National Laboratory, which is supported by the Office of Science of the U.S. Department of Energy under contract DE-AC02-06CH11357. The authors thank GENCI (Grand Equipement National de Calcul Intensif) and CINES (Centre Informatique National de l'Enseignement Superieur) for providing part of the computing power necessary for these simulations. The support of Turbomeca (Dr. C. Berat and Dr. T. Lederlin) is also acknowledged.

REFERENCES

Berkooz, G., Holmes, P. & Lumley, J. L. 1993 The proper orthogonal decomposition in the analysis of turbulent flows. *Ann. Rev. Fluid Mech.* **25**, 539–575.

Dowling, A. P. 1995 The calculation of thermoacoustic oscillations. *J. Sound Vib.* **180** (4), 557–581.

Gourdain, N., Gicquel, L., Montagnac, M., Vermorel, O., Gazaix, M., Staffelbach, G., Garcia, M., Boussuge, J. & Poinsot, T. 2009 High performance parallel computing of flows in complex geometries: I. methods. *Comput. Sci. Disc.* **2**, 015003.

Kaufmann, A., Nicoud, F. & Poinsot, T. 2002 Flow forcing techniques for numerical simulation of combustion instabilities. *Combust. Flame* **131**, 371–385.

Krebs, W., Flohr, P., Prade, B. & Hoffmann, S. 2002 Thermoacoustic stability chart for high intense gas turbine combustion systems. *Combust. Sci. Tech.* **174**, 99–128.

Lieuwen, T., Torres, H., Johnson, C. & Zinn, B. 2001 A mechanism of combustion instability in lean premixed gas turbine combustors. *Journal of Engineering for Gas Turbines and Power* **123** (1), 182–189.

Lieuwen, T. & Yang, V. 2005 Combustion instabilities in gas turbine engines. operational experience, fundamental mechanisms and modeling. In *Prog. in Astronautics and Aeronautics AIAA*, , vol. 210.

Lohrmann, M., Buechner, H. & Zarzalis, N. 2003 Flame transfer function characteristics of swirled flames for gas turbine applications. In *ASME Turbo expo* (ed. A. P. 2003-GT-38113). Atlanta.

Lumley, J. L. 1967 The structure of inhomogeneous turbulence. *Atmospheric Turbulence and Wave Propagation* pp. 166–178.

Mahesh, K., Constantinescu, G., Apte, S., Iaccarino, G., Ham, F. & Moin, P. 2006 Large eddy simulation of reacting turbulent flows in complex geometries. In *ASME J. Appl. Mech.* , , vol. 73, pp. 374–381.

Moin, P. & Apte, S. V. 2006 Large-eddy simulation of realistic gas turbine combustors. *Am. Inst. Aeronaut. Astronaut. J.* **44** (4), 698–708.

Morgans, A. & Dowling, A. 2007 Model-based control of combustion instabilities. *J. Sound Vib.* **299** (1-2), 261 – 282.

Noiray, N., Bothien, M. & Schuermans, B. 2010 Analytical and numerical analysis of staging concepts in annular gas turbines. In *n3l - Int'l Summer School and Workshop on Non-normal and non linear effects in aero and thermoacoustics*.

Poinsot, T. & Lele, S. 1992 Boundary conditions for direct simulations of compressible viscous flows. *J. Comput. Phys.* **101** (1), 104–129.

Poinsot, T., Trouvé, A., Veynante, D., Candel, S. & Esposito, E. 1987 Vortex driven acoustically coupled combustion instabilities. *J. Fluid Mech.* **177**, 265–292.

Poinsot, T. & Veynante, D. 2005 *Theoretical and Numerical Combustion*. R.T. Edwards, 2nd edition.

Roux, A., Gicquel, L. Y. M., Sommerer, Y. & Poinsot, T. J. 2007 Large eddy simulation of mean and oscillating flow in a side-dump ramjet combustor. *Combust. Flame* **152** (1-2), 154–176.

Schmitt, P., Poinsot, T., Schuermans, B. & Geigle, K. P. 2007 Large-eddy simulation and experimental study of heat transfer, nitric oxide emissions and combustion instability in a swirled turbulent high-pressure burner. *J. Fluid Mech.* **570**, 17–46.

Schuermans, B., Bellucci, V. & Paschereit, C. 2003 Thermoacoustic modeling and control of multiburner combustion systems. In *International Gas Turbine and Aeroengine Congress & Exposition, ASME Paper*, , vol. 2003-GT-38688.

Schuermans, B., Paschereit, C. & Monkiewitz, P. 2006 Non-linear combustion instabilities in annular gas-turbine combustors. , vol. AIAA paper 2006-0549.

Selle, L., Lartigue, G., Poinsot, T., Koch, R., Schildmacher, K.-U., Krebs, W., Prade, B., Kaufmann, P. & Veynante, D. 2004 Compressible large-eddy simulation of turbulent combustion in complex geometry on unstructured meshes. *Combust. Flame* **137** (4), 489–505.

Sensiau, C., Nicoud, F. & Poinsot, T. 2009 A tool to study azimuthal and spinning modes in annular combustors. *Int. Journal Aeroacoustics* **8** (1), 57–68.

Staffelbach, G., Gicquel, L., Boudier, G. & Poinsot, T. 2009 Large eddy simulation of self-excited azimuthal modes in annular combustors. *Proc. Combust. Inst.* **32**, 2909–2916.

Stow, S. R. & Dowling, A. P. 2001 Thermoacoustic oscillations in an annular combustor. In *ASME Paper*. New Orleans, Louisiana.

Wolf, P., Staffelbach, G., Roux, A., Gicquel, L., Poinsot, T. & Moureau, V. 2009 Massively parallel les of azimuthal thermo-acoustic instabilities in annular gas turbines. *C. R. Acad. Sci. Mécanique* **337** (6-7), 385–394.